Clinical and Experimental Obstetrics & Gynecology

Clin. Exp. Obstet. Gynecol. **2026**; 53(1): 45631
https://doi.org/10.31083/CEOG45631

Case Report

Case Report of the Identification of a Novel Deep-Intronic *SLC12A1* Variant in a Proband of a Family with Bartter Syndrome for Prenatal Diagnosis

Xiaojia Wu[1], Jianmei Gu[1], Zhen Yang[2], Ping Tang[1,*]

[1]Department of Fetal Medicine, Jiaxing Maternity and Children Health Care Hospital (Affiliated Women and Children Hospital Jiaxing University), 314009 Jiaxing, Zhejiang, China
[2]BGI Genomics, 201321 Shanghai, China
*Correspondence: phoenix@zjxu.edu.cn (Ping Tang)
Academic Editor: Michael H. Dahan
Submitted: 8 August 2025 Revised: 14 September 2025 Accepted: 30 September 2025 Published: 19 January 2026

Abstract

Background: Bartter syndrome (BS) is a rare autosomal recessive genetic disorder, typically characterized by hypokalemic metabolic alkalosis, and sometimes accompanied by hyponatremia and hypochloremia. BS is caused by mutations at multiple gene loci with strong genetic heterogeneity, making accurate genetic analysis crucial for diagnosis. **Case**: We collected peripheral blood samples from three family members: an 8-week pregnant woman, her husband, and their daughter, with BS symptoms. Whole-exome sequencing (WES) and whole-genome sequencing (WGS) were performed, with variants verified by Sanger sequencing. Minigene assays were used to investigate splicing effects, and in silico predictions were conducted to assess the impact of mutations on protein structure. A prenatal diagnosis was performed at 18 weeks of gestation via amniocentesis and Sanger sequencing. **Conclusions**: This case highlights three critical values. First, clinically, WGS provides a feasible solution for diagnosing BS cases with negative WES results, which helps reduce hypokalemia-related complications. Second, this is the first report of the *SLC12A1* c.2961-647T>G and c.1153G>A variants, and integrated validation confirms their pathogenicity, expanding the spectrum of pathogenic *SLC12A1* variants. Third, our findings guide clinicians to consider deep intronic variants and WGS application in unexplained hereditary renal diseases, which is highly relevant to current prenatal diagnosis and genetic counseling practices. WGS can identify deep intronic variants in *SLC12A1*, and functional experiments can strengthen pathogenicity evidence, providing an effective prenatal diagnostic approach for families with a history of BS.

Keywords: bartter syndrome; genetic disease; prenatal diagnosis; whole-genome sequencing; deep intron

1. Introduction

Bartter syndrome (BS) is a rare hereditary renal disorder characterized by tubulopathy leading to electrolyte imbalances, including hypokalemia, metabolic alkalosis, and polyuria, which significantly affect quality of life [1–3]. BS is divided into five subtypes, with types I and II being the most severe, often presenting as an antenatal form of BS [4]. Type I BS is the most common, but the diverse clinical manifestations of this type and similarity to other kidney diseases make diagnosing type I BS challenging [5].

With the development of next-generation sequencing (NGS) technologies, an increasing number of studies have shown that genetic mutations are closely associated with the onset of BS [6,7]. However, BS can be classified into five types depending on the causative gene mutation, with each type associated with a specific gene: solute carrier family 12 member 1 (*SLC12A1*) (MIM600839, type I), inwardly rectifying subfamily J member 1 (*KCNJ1*) (MIM600359, type II), chloride channel, voltage-sensitive Kb (*CLCNKB*) (MIM602023, type III), Barttin (*BSND*) (MIM606412, type IVa), *CLCNKB*, and chloride channel, voltage-sensitive Ka (*CLCNKA*) (MIM602024, type IVb), or melanoma-associated antigen D2 (*MAGED2*) (MIM 300155, type V). Currently, more than 100 mutations in *SLC12A1* have been reported, of which 65 are associated with type I BS and nine are found in the general population and are associated with lower blood pressure levels [8–10]. Common mutations are located in exons and can be detected using the current whole-exome sequencing (WES) techniques. However, conventional WES—focusing on protein-coding regions and flanking splice sites—often fails to detect deep intronic variants (located >20 bp from exons), meaning some cases of BS remain undiagnosed. This diagnostic gap not only delays targeted treatment but also hinders accurate genetic counseling for families. Additionally, the prenatal diagnosis of BS currently lacks clear guidelines for whole-genome sequencing (WGS) applications when WES is negative, leaving clinicians with limited options for managing fetuses with suspected renal abnormalities.

In this case, we used WGS to diagnose a child with suspected BS. Using WGS, we conducted a comprehensive high-throughput analysis of the genome, including both coding and non-coding regions. This allowed us to identify the gene variants associated with BS accurately. This

not only fills the diagnostic gap but also provides clinically relevant evidence for the use of WGS in the prenatal diagnosis of BS.

2. Case Presentation

2.1 Materials and Methods

2.1.1 Sample Collection

This study was approved by the hospital Ethics Committee of Jiaxing Maternal and Child Health Care Hospital (2024-Y-107). Informed consent was obtained from all study participants, and their family members provided written informed consent. Parental consent was obtained for gathering prenatal fetal amniotic cell samples at 18 weeks of pregnancy. Peripheral blood samples were collected from the parents of the proband.

2.1.2 Whole-Genome Sequencing

The polymerase chain reaction (PCR) products were purified and sequenced using BGI Genomics (Shenzhen, Guangdong, China). Candidate mutation sites were identified following DNA extraction, quality inspection, genomic library construction, target-region capture sequencing, and bioinformatic analysis. A total of 500 ng genomic DNA was sonicated, yielding fragments ranging from 250 to 300 bp. After adding a mixture of terminal repair buffer and repair enzyme, the fragments were reacted on a PCR instrument. Then, the end repair system was added to the ligase, buffer, and linker, and the reaction was incubated at 22 °C for 30 minutes. After purification with magnetic beads, the sample mixture was added to the PCR amplification reaction system for 8–10 cycles. After magnetic bead purification, the library quality was assessed: the library was 25 µL, with a concentration >15 ng/µL, an effective molecular concentration >10 nM, and the main DNA fragment peak was at 430 bp, ranging from 300 to 600 bp. Sequencing was performed after finalizing the quality control.

2.1.3 Minigene Assay

The c2961-647T>G mutation was identified in the *SLC12A1* gene. Subsequently, two analysis software tools, RDDC (https://rddc.tsinghua-gd.org) and SpliceAI (https://spliceailookup.broadinstitute.org/), were used to assess the impact of the mutation (*SLC12A1*; c.2961-647T>G) on splicing. The results indicated a positive prediction rate of 90%, suggesting a high likelihood that this mutation influences splicing. Minigene experiments were performed *in vitro*. Normal human genomic DNA (gDNA) was used as a template, and pcMINI and pcMINI-C vector skeletons provided by Baiyi Bio Company (Wuhan, Hubei, China) were used to construct vectors for enzyme digestion, ligation, transformation, and recombinant cloning. The pcMINI-wild-type (wt)/mutant (mut) and pcMINI-C-wt/mut plasmids were used in this study. Minigene fishing and restriction site introduction were also conducted. The recombinant vectors were transiently transfected into HeLa and 293T cells, and samples were collected 48 h after transfection. Total RNA was extracted from the cell samples using a standard liposome-mediated RNA extraction protocol, and the concentration was quantified using a spectrophotometer. Finally, the flanking primers on the minigene vector were used for PCR amplification, and the amplified gene transcript bands were detected by agarose gel electrophoresis. Sanger sequencing was performed on each recovered band.

2.1.4 Protein Structure Prediction

The transmembrane region analysis (TMHMM) website was used to predict the effect of the *SLC12A1* gene c.1153G>A p.Ala385Thr mutation on protein structure.

2.1.5 Fetal Sanger Validation

Sanger sequencing validation of fetal variants was conducted based on whole-genome high-throughput sequencing results, and the PCR products were purified and sequenced on an ABI 3130. National Center for Biotechnology Information (NCBI) Basic Local Alignment Search Tool (BLAST) searches were performed against the human reference genome (hg19) and other reference genomes to identify mutation sites, and the pathogenicity of the variants was determined according to the American College of Medical Genetics and Genomics (ACMG) 2015 genetic variation classification criteria [11]. These variants are classified as pathogenic variants. The ClinGen Working Group on sequence variation Interpretation and the Association for Clinical Genomic Science (ACGS) were referred to for further interpretation of the guidelines.

2.2 Results

2.2.1 Clinical Characteristics

A woman, who was eight weeks pregnant and had previously given birth to a daughter suspected of having BS, was included. In a previous pregnancy, ultrasonography at 28 weeks of gestation revealed an amniotic fluid index of 310 mm, consistent with polyhydramnios. The amniotic fluid level continued to increase progressively, resulting in preterm births at 30 weeks of gestation. The baby girl weighed 1300 g at birth. At the age of 2 years, the daughter developed polydipsia, with a daily water intake exceeding 2500 mL, accompanied by polyuria, with a daily urine volume of 2000 mL (normal range is about 400–600 milliliters/24 hours), as well as nausea and vomiting. Her 24-hour urinary calcium was 175.6 mg (equivalent to 13.5 mg/kg) (normal range is 150–600 milligrams per 24 hours, about 2.5–7.5 millimoles per 24 hours), and her blood potassium level was 2.5 mmol/L (serum potassium level is 3.5–5.5 millimoles per liter). Renal ultrasonography revealed petal-like medullary calcification. The patient is currently on long-term potassium supplementation.

The parents were not consanguineous, had no clinical symptoms, and had normal blood potassium levels. We re-

viewed the medical history, blood test results, and treatment plan of the 8-year-old daughter of the proband, as well as the history of polyhydramnios and preterm birth during the previous pregnancy. The Department of Pediatrics at our hospital confirmed a clinical diagnosis of BS (Fig. 1A).

2.2.2 Whole-Genome Sequencing Identified Pathogenic Genes After Whole-Exome Sequencing Failure

The patient was admitted to the Children's Hospital for suspected BS; however, prior WES performed at other hospitals did not identify pathogenic variants, and a prenatal diagnosis was requested. Therefore, we performed WGS using the total genomic DNA extracted from the proband and his parents. The proband carried a paternal missense mutation (*SLC12A1* c.1153G>A) and maternal splicing variant (*SLC12A1* c.2961-647T>G). We validated these results using Sanger sequencing (Fig. 1B,C). Amniocentesis was used to collect fetal DNA, and Sanger sequencing was performed to verify that the fetus carried the maternal-derived *SLC12A1* c.2961-647T>G variant and that a healthy baby would be born at term. *SLC12A1*; NM_000338.2 : c.2961-647T>G abnormal splicing mutations lead to protein changes and pathogenicity. The evidence item PM2+PS3+PP4 was possibly pathogenic. The *SLC12A1*; NM_000338.2 : c.1153G>A (p.Ala385Thr) evidence item PM2+PM3+PP3+PP4 may also be pathogenic.

2.2.3 Minigene *In Vitro* Experiments

To determine whether this variant causes abnormal splicing of *SLC12A1* and affects the gene expression and function, we performed minigene splicing assays *in vitro*. The software predicted that *SLC12A1* c.2961-647T>G may affect normal mRNA levels, and our experimental results were consistent with this prediction. The electrophoretic patterns of the wt and mut *SLC12A1* gene regions (from exon A to exon 25) showed a difference in bands due to the c.2961-647T>G mutation (Fig. 2A). The reverse transcription-polymerase chain reaction (RT-PCR) results for the wt and mut gene regions in 293T and HeLa cells revealed changes in the band position and intensity of the mutant, suggesting an effect on the transcription products (Fig. 2B). A schematic diagram of the gene structures indicated that the mutant retained intron 24 (188 bp) (Fig. 2C). Electrophoretic patterns of the sequencing results further confirmed the retention of intron 24 in the mutant. Thus, this mutation causes abnormal splicing. The internal retention of intron 24 was 188 bp, and the retention position was c.2961–646_c.2961–459. This retention was expressed at the cDNA and protein levels as follows: c.2960_2961ins GAACCTGAATAATACTCATTTGAAAATCTCAGA CAGCAACATCAAACAACAAAAGGACAAGGGGA GCATTATTTGCAGAAAACGTCCAAATTGTTCTAC AATCATTAAACTTGTGGGAGCCCTTGCTGTTCTC CTCCTACCTGCCCGCGGCCTCCTGCCATGAGTGG GAGTTGCCATGTGGACTAAGG p.Ser987Argfs × 55 (Fig. 2D). Overall, the minigene analysis confirmed that the *SLC12A1* c.2961-647T>G aberrant splicing mutation resulted in a 188 bp retention at intron 24, resulting in a premature stop codon (PTC) and a truncated protein with a size of 1040 aa.

2.2.4 Effect of the Mutation on the Secondary Structure of the SLC12A1 Protein

We compared the differences between wt *SLC12A1* and mutant *SLC12A1* c.1153G>A (p.Ala385Thr) in terms of secondary structure and hydrogen bond distance. In terms of secondary structure, the wt sequence length was 1099 bp, while the mut was also 1099 bp. However, the distribution of the secondary structural elements differed between the two. For example, the wt had 444 amino acids in α-helices, whereas the mutant had 422 amino acids. Moreover, the number of β-sheets, β-turns, random coils, and other structures also differed. In terms of hydrogen bond distances, there were differences between the hydrogen bond distances of Ala385 with other amino acids in the wt and those of Thr385 with corresponding amino acids in the mutant. Some values changed, whereas others presented the same values but involved different amino acids. These structural changes may affect the stability and function of the protein, and may be related to the pathogenesis of relevant diseases (Fig. 3).

2.2.5 Prediction of the Effect of SLC12A1 Mutations on Protein Structure

We identified 385 mutations in the NCBI functional domain database, located in the 2a30 functional domain (https://www.ncbi.nlm.nih.gov/). Using the TMHMM website, the predicted SLC12A1 protein contained 12 transmembrane helices (TMhelix) (Fig. 4), and the mutation at position 385 of the protein was predicted to be located in the transmembrane helix (TMhelix). After the self-optimized method with profile alignment (SOPMA) database analysis, the proportion of alpha helices (Hh), extended strands (Ee), random coils (Cc), and other structures changed, suggesting that the mutation affected the secondary structure. In contrast, the proportions of the structures, such as the beta turn (Tt), 310 helix (Gg), Pi helix (Ii), beta bridge (Bb), bend region (Ss), and ambiguous states, did not change. The c.1153G>A p.Ala385Thr. Alphafold modeling and PyMOL mapping analysis showed that after mutation, the distance of hydrogen bonding between the main chain Thr385 and PHE381 changed, indicating that the mutation may affect the main chain structure of *SLC12A1*. In summary, these mutations may affect the tertiary structure of SLC12A1 (Fig. 4).

2.2.6 Effect of the Mutation on the Surface Potential of the SLC12A1 Protein

We analyzed the structural and surface potential changes in both wild-type and mutant (p.Ala385Thr)

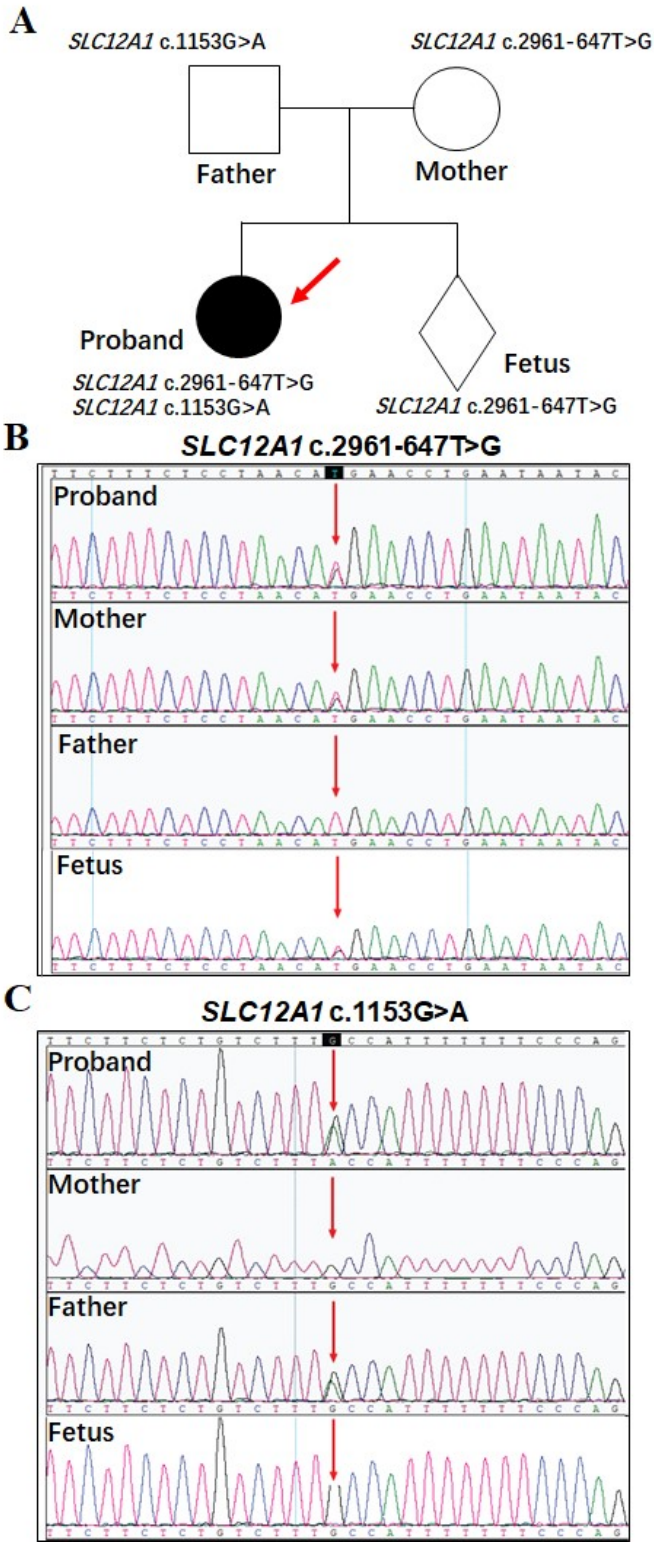

Fig. 1. Identification and analysis of Bartter syndrome-related mutations in a family. (A) Pedigree analysis shows that the proband carries both a paternal missense mutation (*SLC12A1* c.1153G>A) and a maternal splicing variant (*SLC12A1* c.2961-647T>G). The red arrows in panel A point to the proband in the pedigree, clearly indicating the index case of this study. (B) *SLC12A1* c.2961-647T>G variant was verified by Sanger sequencing. The red arrows in panel B highlights the specific nucleotide position (c.2961-647T>G) where the variant occurs, showing the T-to-G nucleotide change compared to the wild-type sequence. (C) *SLC12A1* c.1153G>A variant was verified by Sanger sequencing. The red arrow in panel C highlights specific nucleotide positions (c.1153G>A), where G-to-A nucleotide changes are observed compared to the wild-type sequence.

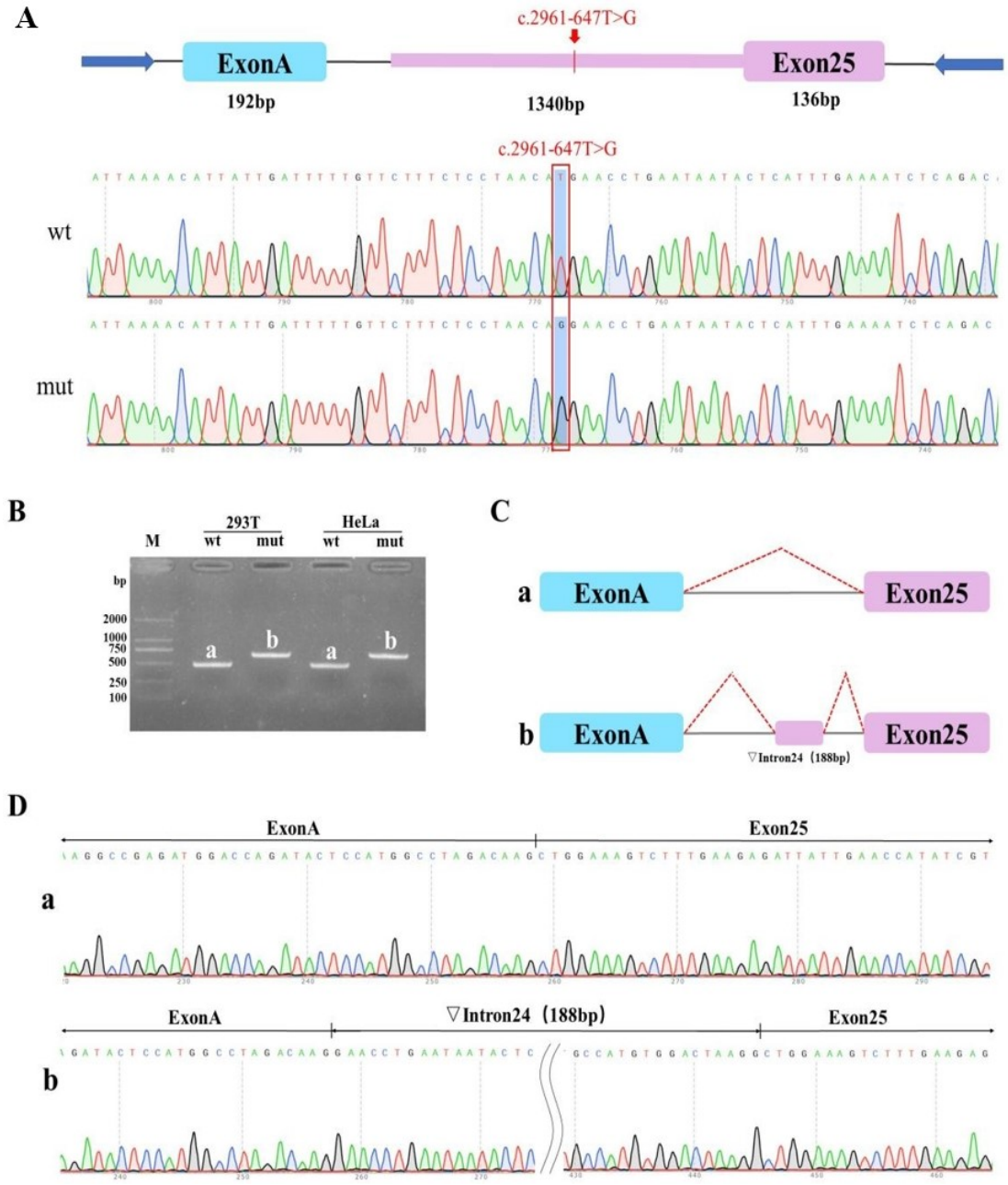

Fig. 2. Analyses of abnormal splicing caused by the *SLC12A1*; c.2961-647T>G mutation. (A) Electrophoretic patterns of the wild-type (wt) and mutant (mut) *SLC12A1* gene region (from exon A to exon 25). The red box (in panel A) encloses the electrophoretic band area of the mutant sample, highlighting the difference from the wild-type band. The red arrow (in panel A) points to the position of the c.2961-647T>G variant, which is a nucleotide substitution site situated within the 1340 bp fragment of intron24. (B) Reverse transcription-polymerase chain reaction (RT-PCR) results of the wt and mut regions in 293T and HeLa cells display changes in band position and intensity for the mutant, indicating an effect on transcription products. (C) A gene structure schematic diagram shows that intron 24 (188 bp) is retained in the mutant. (D) Electrophoretic patterns of the sequencing results confirm the retention of intron 24 in the mutant. Note: "Exon" is the abbreviation of "expression region", referring to the coding sequence region in a gene; terms like "Exon 25" are standard professional expressions in genetics, representing the 25th exon in the gene structure. Specifically, ExonA (Exon A, i.e., expression region A): exhibits a single clear band consistent with the expected size of the target exon, without additional bands indicating intron retention (serving as a normal control); Exon25 (Exon 25, i.e., expression region 25): shows two bands—one matching the normal exon size and another larger band, which is verified to contain the retained intron 24, confirming the splicing abnormality in the mutant.

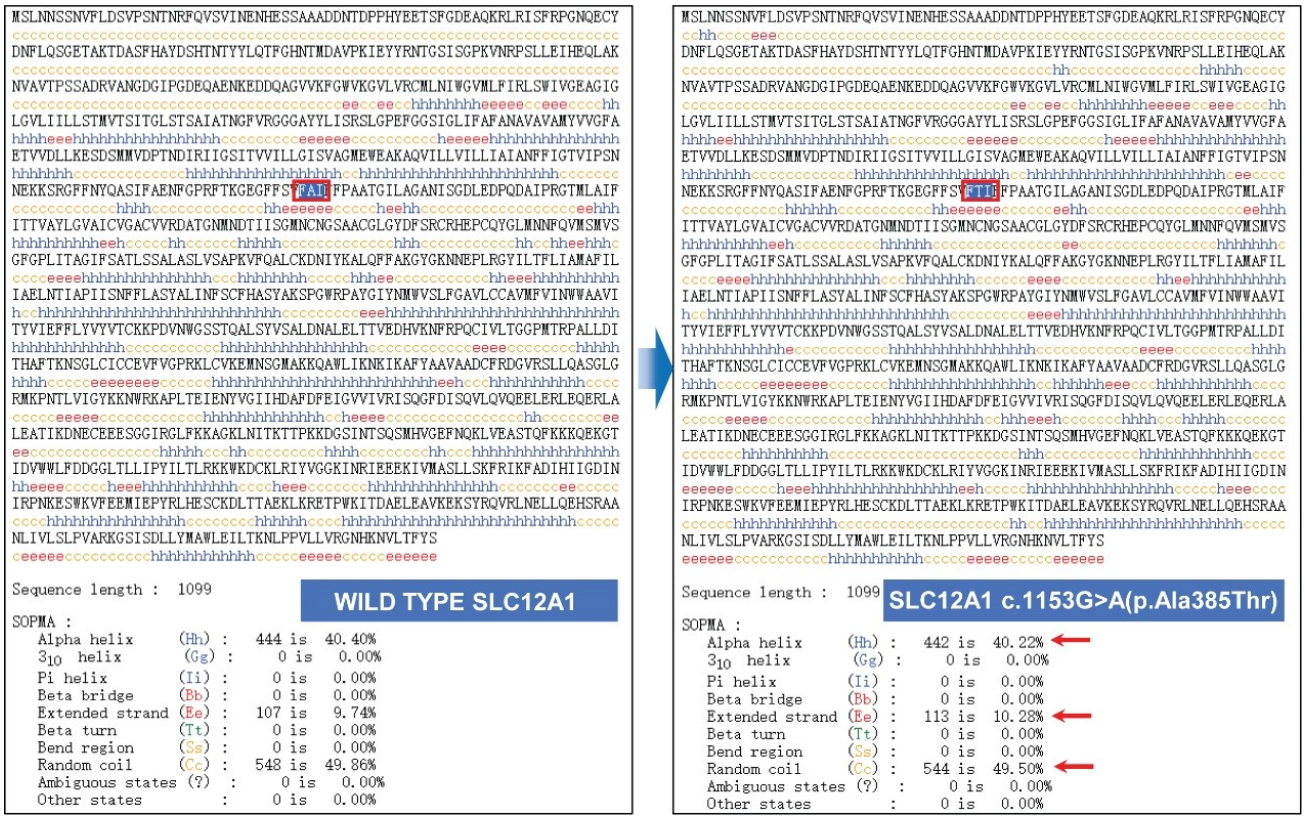

Fig. 3. Effect of genetic variants on the secondary structure of the SLC12A1 protein. This figure compares the secondary structures of the wild-type and mutant (c.1153G>A, p.Ala385Thr) SLC12A1 proteins (both consisting of 1099 amino acids). The red box (in the structural diagram) highlights the region where the secondary structure changes between the wild-type and mutant proteins, while the red arrows point to the specific positions of α-helices/β-sheets that show altered distribution (e.g., reduced α-helix content or increased random coil ratio) in the mutant. These differences in the number of α-helices, β-sheets, β-turns, and random coils may affect the protein's normal function.

SLC12A1 proteins. The wild-type SLC12A1 protein had a specific three-dimensional structure, and a particular surface potential distribution was observed around the locally magnified Ala385. The overall structure of the mutant SLC12A1 protein is similar to that of the wild-type protein. However, owing to the Ala385 to Thr385 mutation, the potential of the local surrounding surface changed significantly. This change in surface potential may affect interactions between the protein and other molecules, thereby influencing the biological functions and related physiological processes of the protein. Fig. 5 demonstrates the potential changes in surface potential of the SLC12A1 protein induced by mutations.

3. Discussion

Pregnant women with BS usually experience polyhydramnios between 18 and 30 weeks of gestation, and their amniotic fluid index can reach 330–500 mm [12,13]. In cases of gestational polyhydramnios, the risk of fetal BS should be considered after excluding pathological conditions such as gestational diabetes. Therefore, this study provides valuable insights. In this case, the patient was a pregnant woman with a history of adverse birth outcomes who required a prenatal diagnosis. After the WES results were negative, WGS was performed to detect two variants of uncertain significance in the *SLC12A1* gene, which is associated with type I BS and was found to be related to the phenotype of the subject. The NM_000338.2: c.2961-647T>G mutation was located in the deep intron region. This may explain why WES failed to identify causative genes and their corresponding variants.

This variant was found to have enhanced pathogenicity through functional verification. Specifically, the corresponding locus of the variant in the *SLC12A1* gene (NM_000338.2: c.1153G>A, p.Ala385Thr) also showed an improved pathogenicity rating. Consequently, this study identified a new *SLC12A1* locus associated with BS. WES is widely used for pediatric and prenatal diagnoses. With the ongoing decline in WES costs and improvements in technology and data analysis, the clinical application of chromosomal chip technology and single-gene sequencing is gradually being replaced [14]. Meanwhile, WES has become the main technological platform for genetic testing. Moreover, deep introns, copy number variations (CNVs),

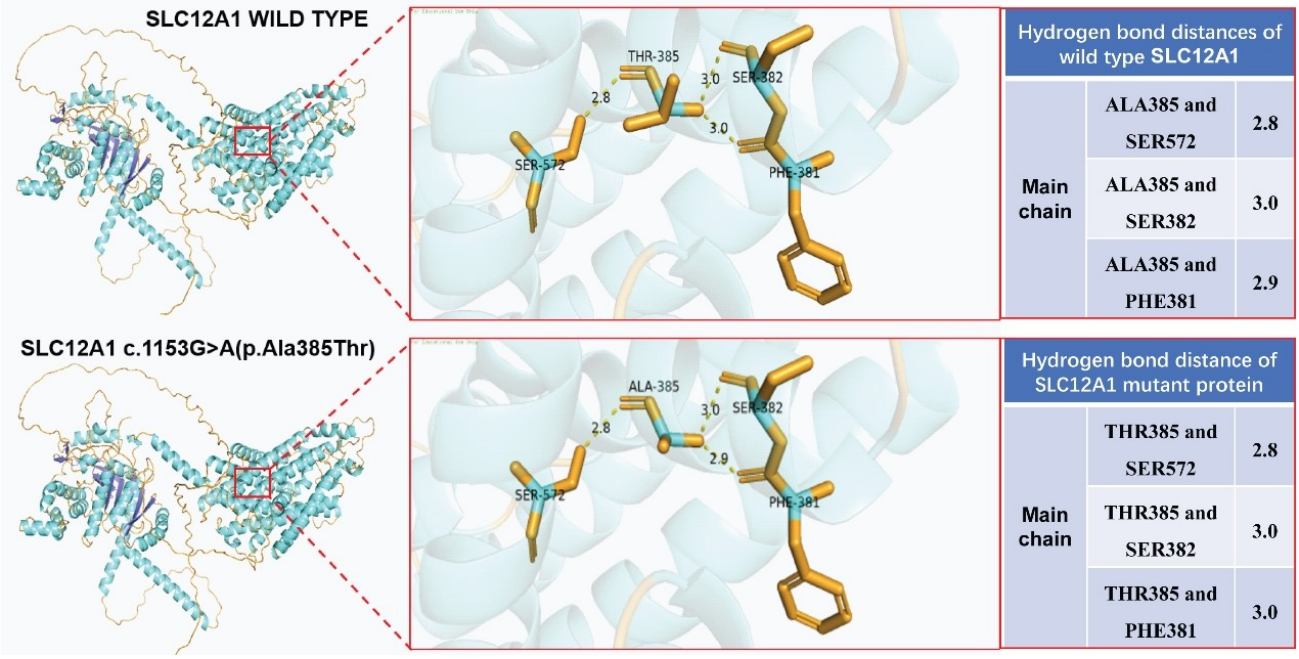

Fig. 4. Effect of genetic variants on the tertiary structure of the SLC12A1 protein. A comparison of the hydrogen-bond distances in wild-type and mutant (c.1153G>A, p.Ala385Thr) SLC12A1 proteins. The hydrogen bond distances related to alanine at position 385 (ALA385) in the wild-type and threonine at position 385 (Thr385) in the mutant differ, which may affect protein-protein interactions. Specifically, the relevant amino acid residues include Phenylalanine 381 (PHE381), Serine 572 (SER572), Serine 382 (SER382), Serine 572 (SER572) and Serine 382 (SER382).

and chromosomal abnormalities cannot be detected because the detection ranges are limited to the exon level [14]. Nonetheless, WGS, based on NGS, is an emerging technology for genetic disease detection that can detect genetic variations, including chromosome numerical abnormalities, genomic variations in copy number, single-nucleotide variations, and small fragment insertions and deletions. High-depth WGS can cover the entire genome, with a wide dynamic range. Simultaneously, this approach can reduce the risk of missed detection to some extent by targeting sequencing or WES library construction. Notably, the current clinical application of WGS still faces practical challenges: clinical laboratories generally have limited experience with WGS, and the use of high-depth WGS (typically defined as a sequencing depth $>30\times$) in clinical settings remains in the early stages. Against this background, our study successfully identified a locus in the intronic region of the *SLC12A1* gene (NM_000338.2: c.2961-647T>G) through peripheral blood testing of a child with suspected BS, which, in turn, provides a foundational basis for subsequent prenatal diagnoses.

Since WGS generates vast amounts of data, more sophisticated bioinformatics analyses are necessary, and genetic variants of uncertain significance have frequently emerged. Currently, the predominant classification criteria and guidelines for genetic variants published in 2015 are used [15]. For Mendelian diseases, a five-level conclusion based on 28 independent evidence judgments was proposed, and a classification system for sequence variants was established.

All compound heterozygous variants of *SLC12A1* detected in this study were initially of uncertain significance and did not provide a basis for prenatal diagnosis. However, after meticulous consultation, functional testing was performed to validate and improve the pathogenicity rating.

SLC12A1 NM_000338.2: c.2961-647T>G variant. Initially classified as a variant of uncertain significance (VUS) according to ACMG guidelines, this variant failed to provide a basis for prenatal diagnosis [15,16]. Therefore, to clarify the pathogenicity of the variant, we conducted meticulous consultations and functional validations, which improved the pathogenicity rating.

The supporting evidence for reclassification includes:

- PP3: Multiple *in silico* analyses (conservation prediction, evolutionary analysis, and splice site impact assessment) consistently predicted harmful effects on the gene or gene product.
- PM2: The variant was absent in normal control populations (Exome Sequencing Project (ESP), 1000 Genomes, and Exome Aggregation Consortium (EXAC) databases) or presented as an extremely low-frequency locus in recessive genetic diseases.
- PS3: *In vitro* minigene assays confirmed that this variant affects *SLC12A1* expression and impairs protein function, consistent with *in silico* predictions that this variant disrupts normal mRNA levels.

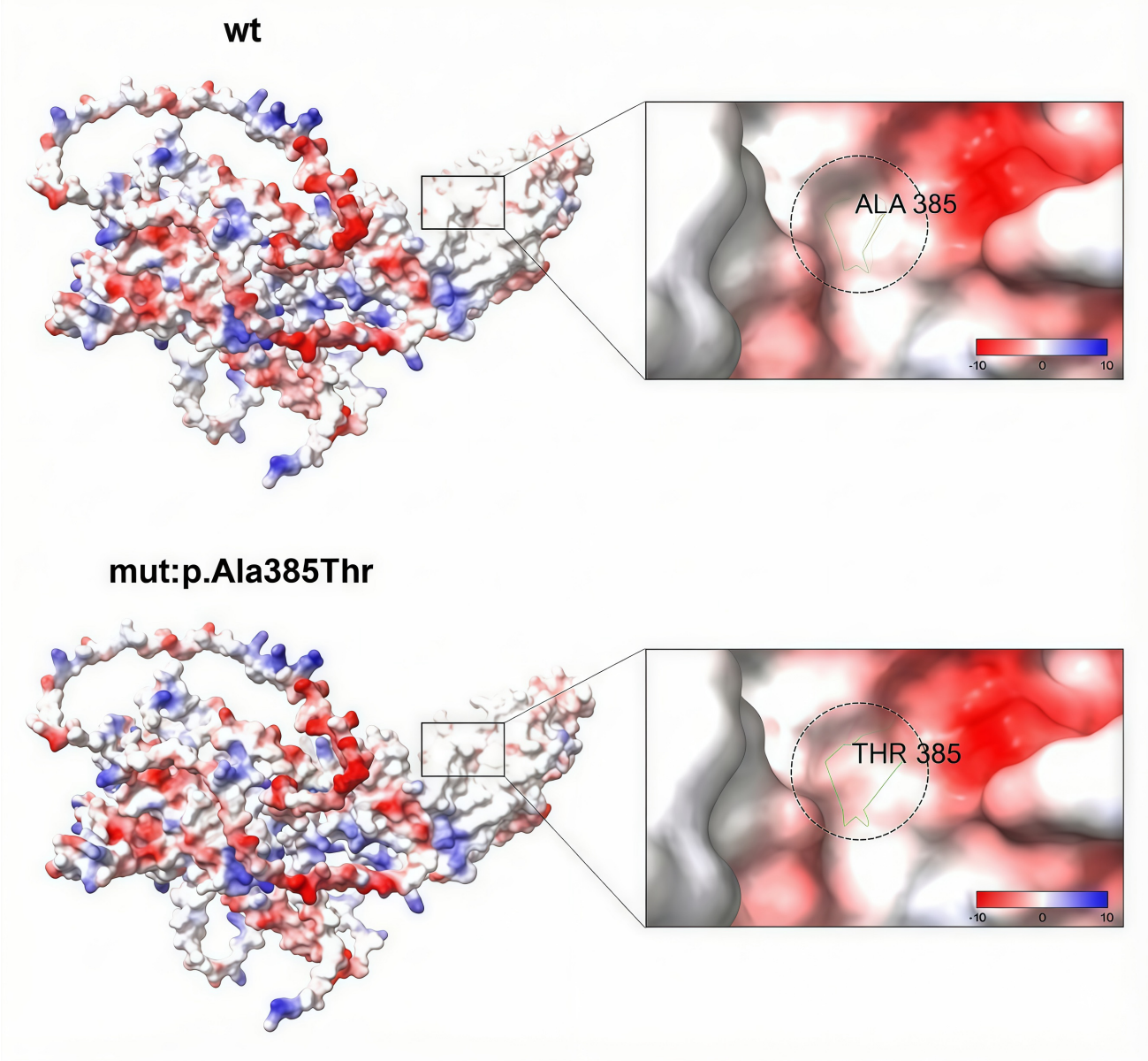

Fig. 5. Surface potential changes in the wild-type and mutant (p.Ala385Thr) SLC12A1 proteins. The results of minigene splicing assays that investigated the effect of the *SLC12A1* c.2961-647T>G variant on gene splicing,including the analysis of Alanine 385 (ALA385) and Threonine 385 (Thr385). The black squares represent the wild-type SLC12A1 protein (Ala385) surface potential values, while the black circles represent the mutant SLC12A1 protein (Thr385) surface potential values.

- PP4: The phenotype and family history of the carrier were highly consistent with a monogenic inherited disorder, supporting the potential pathogenicity of the variant.

Collectively, the evidence (PM2+PS3+PP3+PP4) confirmed the pathogenicity of this intronic variant.

SLC12A1 NM_000338.2: c.1153G>A (p.Ala385Thr) variant. This missense variant was also initially classified as a VUS under ACMG criteria but was re-evaluated through comprehensive analyses [15,16]. Key evidence for the pathogenicity of this variant includes:

- PP3: *In silico* predictions (conservation, evolutionary, and splice site impact analyses) indicate harmful effects on the gene product.
- PM2: The variant was not detected in normal control databases (ESP, 1000 Genomes, EXAC) or exhibited extremely low frequency in recessive disease cohorts.
- PM3: In the context of recessive inheritance, the variant was identified in trans with another pathogenic allele.
- PP4: The phenotype and family history of the carrier were highly consistent with a monogenic disorder, reinforcing the clinical relevance of the variant.

Functional assessments further demonstrated that the c.1153G>A mutation alters the protein structure. Combined with the clear clinical diagnosis, the cumulative evidence (PM2+PM3+PP3+PP4) supported the pathogenicity of the variant.

Given the stringency required for the prenatal diagnosis, clarifying the pathogenicity of these *SLC12A1* variants through systematic validation provides a critical basis for accurate prenatal risk assessment.

Given the particularities of prenatal diagnosis, identifying the mutation sites of pathogenic genes and their pathogenicity requirements remains necessary [17]. Therefore, we performed functional tests to clarify the significance of the pathogenicity. Presently, mutations that affect splicing are often tested for protein function, while protein structure is predicted using software that does not affect splicing. However, the evidence items are frequently not accepted. Similar to *SLC12A1*, NM_000338.2: c.2961-647T>G deep intron variations can lead to protein truncation and pathogenicity. Upgrading of the *SLC12A1* c.1153G>A missense mutation is also caused by variations in the contralateral nucleotide chain.

Limitations and Future Perspectives

3.1.1 Sample Size and Generalizability of Conclusions

As a single case report, although the novel deep intronic *SLC12A1* variant identified here was validated by WGS (after WES failure) and supported by functional assays, the rarity of this variant and the uniqueness of the genetic background of the patient limit the generalizability of our findings. We cannot conclude whether this variant is a common pathogenic cause of BS in broader populations, nor can we confirm its genotype–phenotype correlation in other patients with similar clinical manifestations. Hence, future studies with larger cohorts (e.g., multi-center case series) are needed to verify the prevalence and clinical significance of this variant.

3.1.2 Scope of Genomic Sequencing and Variant Interpretation

WGS successfully identified the deep intronic variant missed by WES. However, we did not systematically explore other non-coding regulatory regions that might also contribute to the pathogenesis of BS. Additionally, due to a lack of population frequency data for this specific deep intronic variant, we could not fully exclude the possibility of rare benign variation, despite the predicted pathogenicity of the variant by *in silico* tools and functional experiments.

3.1.3 Depth of Functional Validation and Structural Modeling

Our functional assays (e.g., minigene experiments) confirmed the pathogenic effect of the variant on *SLC12A1* function; however, these assays did not provide direct structural validation of the protein (e.g., via X-ray crystallography or cryo-EM). These limitations mean that the specific molecular mechanism through which the variant disrupts *SLC12A1* function remains partially unclear.

To address the above limitations, future research should focus on two aspects: (1) Expanding the cohort to include more patients with BS who tested negative for WES, to explore the prevalence of deep intronic *SLC12A1* variants and the associated genotype–phenotype correlations; (2) performing functional experiments in renal tubule-specific cell models to better simulate *in vivo* conditions.

4. Conclusions

Our case underscores one key clinical value of WGS-based diagnosis for BS: this study optimizes prenatal genetic counseling. Before the WGS results, the family faced uncertainty about the condition of the fetus (e.g., "whether the renal abnormality was genetic" or "whether future pregnancies would be at risk"). WGS can effectively identify deep intronic variants in *SLC12A1*, and functional experiments can provide critical evidence for the pathogenicity of the variant. The identification of the *SLC12A1* variant allowed us to inform the family of the autosomal recessive inheritance pattern (both parents were found to be carriers via subsequent testing) and to offer an effective prenatal diagnostic approach for families with a history of BS.

Our findings are highly relevant to current clinical practice and research: For clinicians (especially neonatologists and prenatal diagnosticians), our case provides a "clinical algorithm" reference: when a patient presents with clinical features of BS (e.g., renal salt wasting, hypokalemia) but WES is negative, deep intronic variants should be considered, and WGS should be recommended as the next step. This directly addresses a common clinical dilemma and helps reduce misdiagnosis. For prenatal diagnosis programs, our case provides real-world evidence for incorporating WGS into the diagnostic workflow of suspected BS.

Abbreviations

PM2, Pathogenic Moderate evidence 2; PM3, Pathogenic Moderate evidence 3; PP3, Pathogenic Supporting evidence 3; PP4, Pathogenic Supporting evidence 4; PS3, Pathogenic Strong evidence 3; BS, Bartter syndrome; WGS, whole-genome sequencing; VUS, variants of uncertain significance; NGS, next-generation sequencing; ACMG, American College of Medical Genetics and Genomics; ACGS, the Association for Clinical Genomic Science; PTC, premature stop codon; WES, Whole-exome sequencing; CNV, copy number variations; TMHMM, Transmembrane Protein Homology Model; TMhelix, transmembrane helices; Hh, alpha helices; Ee, extended strands; Cc, random coils; Tt, beta turn; Gg, 310 helix; Ii, Pi helix; Bb, beta bridge; Ss, bend region.

Availability of Data and Materials

All data generated or analyzed during this study are included in the article. Additional raw/processed data supporting the conclusions of this article will be shared by the lead contact upon reasonable request. The charts presented in this manuscript are original works of the authors, have not been previously published, and do not involve third-party copyrights. The dataset used in the current research is available from the corresponding author upon reasonable request.

Author Contributions

XW designed this study. XW, ZY and JG conducted research. PT provided critical guidance on the study design, offered in-depth suggestions on the research protocol optimization, and provided substantial editorial advice on the manuscript structure, logical framework, and academic expression during the writing process. XW analyzed these data. XW and JG jointly wrote the manuscript. All authors contributed to editorial changes in the manuscript. All authors read and approved the final manuscript. All authors have participated sufficiently in the work and agreed to be accountable for all aspects of the work.

Ethics Approval and Consent to Participate

The study was carried out in accordance with the guidelines of the Declaration of Helsinki. Received approval from the Prenatal Diagnosis Ethics Committee at the Maternal and Child Health Care Hospital of Jiaxing, Zhejiang, China (Ethic Approval Number: 2024-Y-107), and all of the participants provided signed informed consent.

Acknowledgment

Special thanks to the staff of the Prenatal Diagnosis Laboratory at Jiaxing Maternal and Child Health Hospital for providing technical assistance in sample sequencing. We also appreciate the constructive comments from the reviewers, which greatly improved the quality of this manuscript. Finally, we would like to express our gratitude to all the research participants for their collaboration.

Funding

This study was also funded by Project of Science and Technology Bureau of Jiaxing, China (2022AY10028); Medical and Health Technology Project of Zhejiang, China (2023KY1220).

Conflict of Interest

The authors declare that they have no affiliations with or involvement in any organization or entity with any financialinterest in the subject matter or materials discussed in this manuscript. As a third-party company, BGI Genomics did not participate in the preparation and publication of the manuscript.

Declaration of AI and AI-Assisted Technologies in the Writing Process

During the preparation of this work the authors used ChatGpt-3.5 in order to check spell and grammar. After using this tool, the authors reviewed and edited the content as needed and takes full responsibility for the content of the publication.

Supplementary Material

Supplementary material associated with this article can be found, in the online version, at https://doi.org/10.31083/CEOG45631.

References

[1] Bartter FC, Pronove P, Gill JR, Jr, Maccardle RC. Hyperplasia of the juxtaglomerular complex with hyperaldosteronism and hypokalemic alkalosis. A new syndrome. The American Journal of Medicine. 1962; 33: 811–828. https://doi.org/10.1016/0002-9343(62)90214-0.

[2] Watanabe S, Fukumoto S, Chang H, Takeuchi Y, Hasegawa Y, Okazaki R, *et al*. Association between activating mutations of calcium-sensing receptor and Bartter's syndrome. Lancet. 2002; 360: 692–694. https://doi.org/10.1016/S0140-6736(02)09842-2.

[3] Gaggar P, Raju DSB, Tej MR, Pragna P. Late-Onset Bartter's Syndrome Type II with End-Stage Renal Disease Due to a Novel Mutation in KCNJ1 Gene in an Indian Adult Male - A Case Report. Indian Journal of Nephrology. 2023; 33: 57–60. https://doi.org/10.4103/ijn.ijn_383_21.

[4] Mrad FCC, Soares SBM, de Menezes Silva LAW, Dos Anjos Menezes PV, Simões-E-Silva AC. Bartter's syndrome: clinical findings, genetic causes and therapeutic approach. World Journal of Pediatrics. 2021; 17: 31–39. https://doi.org/10.1007/s12519-020-00370-4.

[5] Gross I, Siedner-Weintraub Y, Simckes A, Gillis D. Antenatal Bartter syndrome presenting as hyperparathyroidism with hypercalcemia and hypercalciuria: a case report and review. Journal of Pediatric Endocrinology & Metabolism. 2015; 28: 943–946. https://doi.org/10.1515/jpem-2014-0188.

[6] Choi N, Kang HG. Bartter Syndrome: Perspectives of a Pediatric Nephrologist. Electrolyte & Blood Pressure. 2022; 20: 49–56. https://doi.org/10.5049/EBP.2022.20.2.49.

[7] Nojehdeh ST, Mojbafan M, Hooman N, Hoseini R, Otukesh H. Genetic diagnosis of Bartter syndrome in Iranian patients and detection of a novel homozygous *CLCNKB* mutation. Clinical Case Reports. 2022; 10: e6698. https://doi.org/10.1002/ccr3.6698.

[8] Ji W, Foo JN, O'Roak BJ, Zhao H, Larson MG, Simon DB, *et al*. Rare independent mutations in renal salt handling genes contribute to blood pressure variation. Nature Genetics. 2008; 40: 592–599. https://doi.org/10.1038/ng.118.

[9] Brochard K, Boyer O, Blanchard A, Loirat C, Niaudet P, Macher MA, *et al*. Phenotype-genotype correlation in antenatal and neonatal variants of Bartter syndrome. Nephrology, Dialysis, Transplantation. 2009; 24: 1455–1464. https://doi.org/10.1093/ndt/gfn689.

[10] Konrad M, Nijenhuis T, Ariceta G, Bertholet-Thomas A, Calo LA, Capasso G, *et al*. Diagnosis and management of Bartter syndrome: executive summary of the consensus and recommendations from the European Rare Kidney Disease Reference Network Working Group for Tubular Disorders. Kidney International. 2021; 99: 324–335. https://doi.org/10.1016/j.kint.2020.

10.035.
[11] Richards S, Aziz N, Bale S, Bick D, Das S, Gastier-Foster J, *et al*. Standards and guidelines for the interpretation of sequence variants: a joint consensus recommendation of the American College of Medical Genetics and Genomics and the Association for Molecular Pathology. Genetics in Medicine. 2015; 17: 405–424. https://doi.org/10.1038/gim.2015.30.
[12] Fretzayas A, Gole E, Attilakos A, Daskalaki A, Nicolaidou P, Papadopoulou A. Expanding the spectrum of genetic mutations in antenatal Bartter syndrome type II. Pediatrics International. 2013; 55: 371–373. https://doi.org/10.1111/j.1442-200X.2012.03716.x.
[13] Legrand A, Treard C, Roncelin I, Dreux S, Bertholet-Thomas A, Broux F, *et al*. Prevalence of Novel *MAGED2* Mutations in Antenatal Bartter Syndrome. Clinical Journal of the American Society of Nephrology. 2018; 13: 242–250. https://doi.org/10.2215/CJN.05670517.
[14] Kaname T, Yanagi K, Naritomi K. A commentary on the promise of whole-exome sequencing in medical genetics. Journal of Human Genetics. 2014; 59: 117–118. https://doi.org/10.1038/jhg.2014.7.
[15] Anderson JA, Hayeems RZ, Shuman C, Szego MJ, Monfared N, Bowdin S, *et al*. Predictive genetic testing for adult-onset disorders in minors: a critical analysis of the arguments for and against the 2013 ACMG guidelines. Clinical Genetics. 2015; 87: 301–310. https://doi.org/10.1111/cge.12460.
[16] Hegde M, Ferber M, Mao R, Samowitz W, Ganguly A, Working Group of the American College of Medical Genetics and Genomics (ACMG) Laboratory Quality Assurance Committee. ACMG technical standards and guidelines for genetic testing for inherited colorectal cancer (Lynch syndrome, familial adenomatous polyposis, and MYH-associated polyposis). Genetics in Medicine. 2014; 16: 101–116. https://doi.org/10.1038/gim.2013.166.
[17] Chu G, Li P, Wen J, Zheng G, Zhao Y, He R. Copy Number Variation Analysis of 5p Deletion Provides Accurate Prenatal Diagnosis and Reveals Candidate Pathogenic Genes. Frontiers in Medicine. 2022; 9: 883565. https://doi.org/10.3389/fmed.2022.883565.